
Citation:

Marino, MD (2013) RFiof: An RF Approach to I/O-pin and Memory Controller Scalability for Off-chip Memories. In: Proceedings of the ACM International Conference on Computing. UNSPECIFIED. ISBN 978-1-4503-2053-5 DOI: <https://doi.org/10.1145/2482767.2482803>

Link to Leeds Beckett Repository record:

<https://eprints.leedsbeckett.ac.uk/id/eprint/1874/>

Document Version:

Book Section (Accepted Version)

The aim of the Leeds Beckett Repository is to provide open access to our research, as required by funder policies and permitted by publishers and copyright law.

The Leeds Beckett repository holds a wide range of publications, each of which has been checked for copyright and the relevant embargo period has been applied by the Research Services team.

We operate on a standard take-down policy. If you are the author or publisher of an output and you would like it removed from the repository, please [contact us](#) and we will investigate on a case-by-case basis.

Each thesis in the repository has been cleared where necessary by the author for third party copyright. If you would like a thesis to be removed from the repository or believe there is an issue with copyright, please contact us on openaccess@leedsbeckett.ac.uk and we will investigate on a case-by-case basis.

RFiof: An RF Approach to I/O-pin and Memory Controller Scalability for Off-chip Memories

ABSTRACT

Given the maintenance of Moore's law behavior, core count is expected to continue growing, which keeps demanding more memory bandwidth destined to feed them. Memory controller (MC) scalability is crucial to achieve these bandwidth needs, but constrained by I/O pin scaling. In this study, we introduce RFiof, a radio-frequency (RF) memory approach to address I/O pin constraints which restrict MC scalability in off-chip-memory systems, while keeping inter-connection energy at lower levels.

In this paper, we model, design, and demonstrate how RFiof achieves high MC I/O pin scalability for different memory technology generations, while evaluating its area and power/energy impact. By introducing the novel concept of RFpins – to replace traditional MC I/O pins, using RFMCs - MCs coupled to RF transmitters (TX) / receivers (RX), while employing a minimal RF-path between RFMC and ranks, we demonstrate that for a 32-out-of-order multicore configured with off-chip DDR3-ranks with a 1:1 core-to-MC ratio, RFiof presents a scalable 4-RFpin-magnitude per RFMC - comparable to pin-scalable optical solutions - and is able to respectively improve bandwidth and performance by up to 7.2x and 8.6x, compared to the traditional baseline – constrained to MC I/O pin counts. Furthermore, RFiof reduces about 65.6% of MC area usage, and 80% of memory-path energy interconnection.

1. INTRODUCTION

Higher transistor densities described by Moore's law have been pushing core-count growth along different processor generations. As a result of the core count growth, memory pressure increases due to the higher contention, i.e., while subject to larger latencies, less bandwidth is available to the cores - likely decreasing the performance. For example, given the currently largest multi and manycores are in the 16-256 core-range, and the expected core-count growth in next processor generations, scalable memory systems are required to supply appropriate bandwidth to them.

To be able to provide enough bandwidth, typical adopted solutions are based on faster and larger memory-width, keeping the same levels of MC I/O pin counts - in this paper, simply I/O pins or pins. Typical solutions are DDR-based, employed in PCs, tablets, cellphones, GPUs, and others. These DDR- solutions are cost-effective design alternatives when pin-count and MC-count are kept at low levels.

As core-counts grow, we observe that these DDR solutions, as illustrated in Figure 1a, are bound by I/O pin constraints – reported in ITRS [13] as higher I/O pin density per unity of area and total amount of I/O pins - restricting memory bandwidth improvement via MC scalability. Furthermore, although 3D-stack memories eliminate the need of I/O pins, allowing larger memory parallelism via MC scalability, researchers [11] report that rank stacking create restrictions to dissipate heat. Thus, it is fundamental to search off-chip memory solutions which are pin- and MC-scalable.

We point that high-bandwidth off-chip MC-scalable solutions employ telecommunication mechanisms coupled with a low latency media in order to address I/O pin scalability restrictions. For example, optical and wired-RF - or sim-

ply RF - solutions [7][39] respectively employ frequency division multiplexing mechanisms (known as wavelength division multiplexing in optics), and fiber/RF transmission lines in order to reduce I/O pin counts, thus allowing MC scalability. More commercial solutions such as Intel FBDIMM employ serialization [12], which is also used in RAMBUS XDR2 [33] in addition to equalization. However, as DDR memories, these two commercial techniques are neither pad/pin scalable and nor present bandwidth per pad/pin comparable to optical-MC or RFMC scalable systems [7][39]. Reports [20][21][35] show that RF-systems present significant lower development cost, lower temperature sensitivity, and lower-power utilization when compared to optics ones.

In order to address multicore I/O pin scaling demands, in this paper we introduce RFiof, a novel RF-memory approach aiming a pin- and MC-scalable, while power-efficient, and provides an RF direct minimal interconnection between processor and ranks, as illustrated in Figure 1b. We create an RFiof model and evaluate it with several memory bandwidth-bound benchmarks using accurate simulation tools.

In RFiof, as a replacement of the traditional I/O pin, we introduce the novel concept of RFpin. RFpins satisfy the requirements of working at RF-range of frequencies, minimizing the number of elements employed along the RF memory path, and being scalable. To satisfy these RF requirements, in RFiof we have selected similar RF structures to the ones proposed by Lameris et al. [17], which employ a microstrip¹ and a microstrip-to-trench interface - both composing what we define as an RFpin, and a coaxial cable [17]. To satisfy the requirements of scalability, we propose to extend Lameris' design [17] to fit multiple RFMCs and ranks. To the best of our knowledge, the proposed set is for the first time employed to reduce I/O pin counts. We observe that these structures are an electric alternative, while symmetrical to optical systems, such as Corona [7]: optical-MCs, optical TX/RX, fiber, and optical rank, versus RFMCs, RF TX/RX, coaxial cable, and a traditional electrical-rank.

In this paper, we present the design, modeling, viability, and analysis of RFiof in terms of RFpins and RFMC scalability for future technology nodes and different commercial memory generations, comparing it to the traditional electrical-based MC-DRAM path. In addition, as a high-bandwidth solution, we perform an analysis of how RFiof explores modulation, high-frequencies, RF circuitry, and area. Using ITRS [13] predictions, RF [20][21][35] technology predictions, and real RF [17][25] elements, we show that while DDR-compatible, RFpins match different generations of rank bandwidth demands, and most importantly, RFpins are scalable being able to address I/O pin limitations: having Corona [7] as baseline, RFiof is count comparable - 4-RFpin per rank, and have significant lower pin usage than RAMBUS XDR2 [33] and Intel FBDIMM [12] memory systems.

Considering standard server motherboards dimensions and the fact that the use of an auxiliary memory board is likely to increase power, chassis size, cooling, and manufacturing costs, we restrict RFMC scalability investigation to 32 cores:

¹Generally employed in RF-chip communications and composed by a trace of metal on top of a substrate.

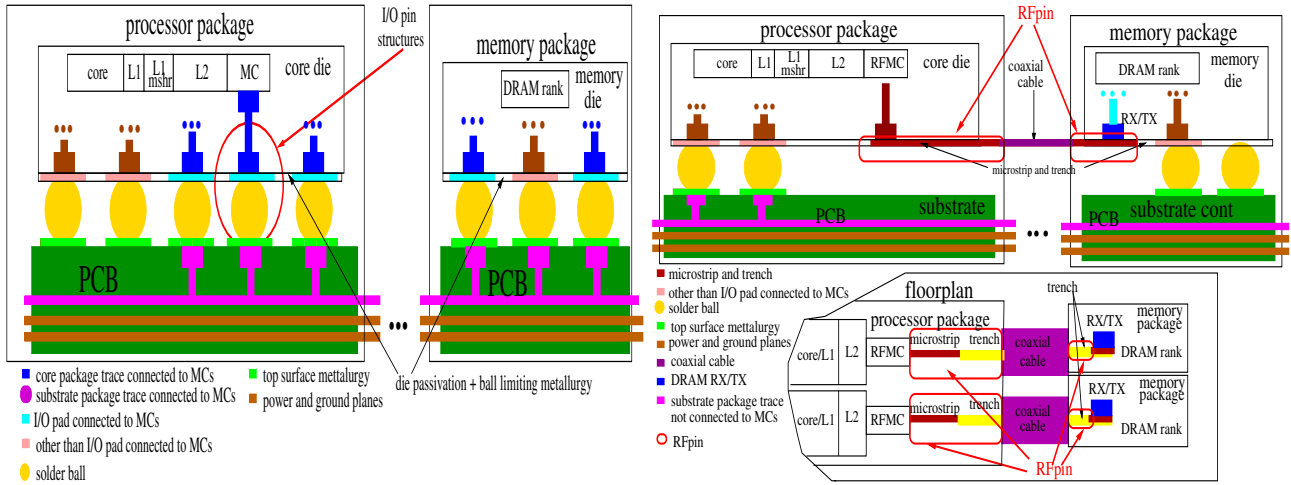


Figure 1: left: a. traditional memory path; right b. RFiof memory path;

for a 32-core-processor we examine up to 32 RFMCs, or alternatively, core:MC ratios from 1:32 to up to 1:1.

Given that RFpins are scalable, we demonstrate architectural RFMC scalability and latency benefits, as well as its performance effects in two independent but complementary ways: (a) memory parallelism benefits through the use of RFpins; (b) latency improvements when transferring bursts and memory commands at the speed of light [34], i.e., by reducing the wire delays between the RFMC and rank. Having a MC-baseline correspondent to an electrical-based version with I/O pins scaled under ITRS I/O pin constraints, our findings show that employing standard 1333 MT/s DDR3 ranks (Table 2 contains the complete settings) interfaced to appropriated RF TX/RX, RFMC scaling and RF latency benefits improve bandwidth and performance respectively by a factor of 7.2x and 8.6x, when compared to the baseline. Moreover, since bandwidth and (b) latency are directly related, we observe around 69% of latency reduction.

To evaluate RFiof area and power benefits, we employ the methodology proposed in [24], which evaluates the architectural benefits of replacing MCs with RFMCs. As a result, we observe a MC area saving benefit of up to 65.6%, which can be alternatively seen as replacing each MC with 2.8 RFMCs, thus allowing larger RFMC scalability and improving bandwidth. Furthermore, we show that MC I/O pads are eliminated in RFiof, which may reduce chip-fabrication costs as a consequence of MC I/O pad area reduction. In terms of power / energy, our findings show that replacing MCs with RFMCs can save up to 80% of interconnection energy. This paper is organized as follows: section 2 discusses the I/O pin problem. Section 3 presents RFiof, compares it to traditional, and to high-scalable pin solutions. Section 4 presents the experiments and results. Section 5 presents the related work, and section 6 concludes it.

2. THE I/O PIN PROBLEM AND SCALABLE SOLUTIONS

Through this sequence of experiments, we illustrate how the I/O pin problem limits bandwidth in regards to pin counts. Furthermore, we show why current solutions are not scalable, and what is behind high-bandwidth I/O pin scalable solutions such as RF, optical, and 3Dstacking.

2.1 Background/Motivation: The I/O pin problem

We start briefly listing the representative background rea-

son elements of the I/O pin problem: (i) electromigration at higher clock rates and pitch size densities; (ii) crosstalk due to likely higher route densities [13]; (iii) giving smaller dimensions, an I/O-pad-to-PCB-pad reliable connection is likely to be challenging. All three aspects affect bandwidth.

Before describing the motivations for higher pin / bandwidth demands, we first define the electrical baseline MC-count, using the scaling predictions of MC/pin counts versus MC-count by Polka [1] and ITRS [13], as well as current 16-core-4MC-AMD Bulldozer processor. We conclude that 32-core OOO processors are likely to have 5 MCs (32:5 core-to-MC ratio), defined as the baseline MC-count.

To investigate the I/O pin problem, we employ the methodology proposed by Marino [22], not to I/O pads, but to I/O pins, which consists comparing the potential performance of RFiof with RFpins – obtained at 1:1 core:MC ratio, with the baseline under MC I/O pin constraints, in two experiments. (i) the bandwidth of one rank is obtained to proper calibrate the system; (ii) the first experiment is extended from 32:1 up to 32:32 core:MC ratios (32:32 equivalent to 1:1), by proportionally increasing I/O pin counts with MC counts. Then, bandwidth and MC I/O pin usage of these core:MC ratio ranges are obtained and compared to the baseline ones.

Before summarizing the experiments, we point that we have selected a generic DDR3 memory rank employed in PCs, (64 data bits, 1333 Mtransactions/s or MT/s) based on the Micron model MT41K128M8 of 1GB [28], described in table 2. The two experiments were modeled employing M5 [30] and DRAMsim [8] simulators, with the following settings: (i) a bandwidth measurement using STREAM memory intensive benchmark [26] (table 3) is experimented for a set formed by one core (1 core, 4.0 GHz 4-wide OOO core, one MC at 4.0GHz), one crossbar with 1-cycle latency – further described in table 2, and one MC connected to just one rank (to extract its maximum bandwidth); (ii) this set configuration is extended to a 32-core system with core:MC proportions varying from 32:1 to 32:32 (or 1:1).

Experiment (i) reports an average memory bandwidth of 2.5 GBytes/s for one rank, which confirms its proper [28] calibration. In experiment (ii), as illustrated in Figure 2, our findings show that the 1:1 core:MC ratio has about 6x larger bandwidth magnitude than the 32:5 core:MC baseline ratio, which motivates the search for addressing RFMC scalability. As a result of Micron manuals' investigation [28], we observe that 50% of the module pins are destined to power purposes while the other 50% for the rest of signals, i.e., 120 pins

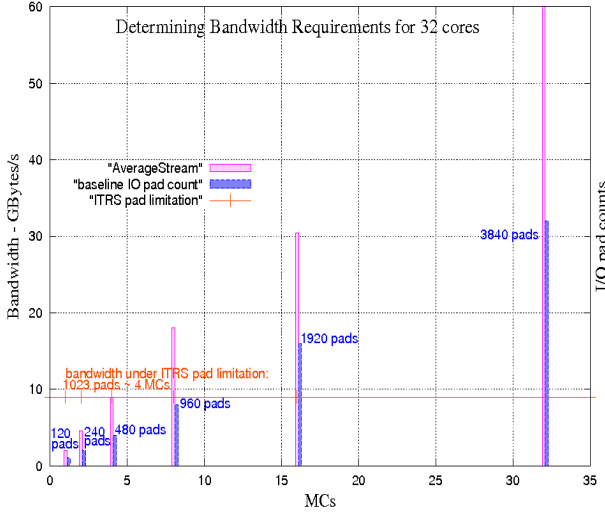


Figure 2: bandwidth demand for 1:1 core-to-MC ratio for 32 cores and I/O pin counts

are dedicated to control/data/address signals (240 on total). Regarding I/O pin usage, Figure 2 presents the result of experiment (ii) with different core:MC ratios and shows that employing 32 ranks would require $32 * 240 = 7840$ pins, which is a significant amount, and if used would require larger package area, routing, and costs.

Additionally, other examples [3][4][6][10][36] of significant pin/MC counts are AMD Bulldozer-4 MCs/2000pins, NVidia GT200 - 8MCs/2495pins, Tiler TILE64 - 4MCs/1500pins, and finally the 192-core Cisco-IBM CRS-1 router - 16 MCs.

2.2 Current memory solutions do not scale

We define the bandwidth per pin as:

$$bw_pin = bandwidth_rank / number_of_IO_pins \quad (1)$$

Typical DDR-family design involves the utilization of wider buses and larger clock frequencies - both as numerator parameters of (1) - to achieve high bandwidth per pin. Moreover, using the 180-240 I/O pins/MC range and typical 17GB/s-data-rate reported by Polka [1] as inputs to equation (1), it produces a low-magnitude bandwidth per pin of 2Gbits/s/pin. Intel FBDIMM [12] employs a pair of serial differential short-wide high-speed busses to connect MC and a cache buffer (responsible for a large power consumption) placed at the ranks to achieve 48 pins/MC and a 2.5Gbits/s/pin-data-rate, while RAMBUS XDR2 [33] uses a high speed serial signaling with adaptive equalization (by removing the signal resistor-capacitor component over serial transmission) to achieve 32 pins/MC and a 12.8 Gbits/s/pin-data-rate [33]. We observe that these two commercial solutions provide larger bandwidth per pin and reduced pin usage than DDR memories, however their still significant I/O pin-count magnitudes do not allow MC scalability, which triggers the search for high-pin-scalable mechanisms.

2.3 Pin-scalable: Optical and RF

We note that general mechanisms that contribute to high-pin scalability are not only exclusive to optics [7], but also of RF [22]. Researchers report [34] that in RF, signals travel at close-to-light speed, with significant low-magnitude energy utilization for 1mm-30cm distance-range [20][35], and, as in optics, Frequency Division Multiplexing mechanism (FDM - data are carried by different frequency bands) is employed. Finally, to the previously mentioned factors, its lower costs

and CMOS fabrication maturity aspects mentioned in [35] favors RF comparatively to optics.

Since high pin-scalable solutions use modulation, we incorporate this mechanism into equation (1):

$$bw_pin = n_{carrier} * data_rate / number_of_IO_pins, \quad (2)$$

Using Corona [7] scalable 2-I/O-optical-pins per MC and its wavelengths (carriers), we have:

$$bw_pin = 160GBytes/s/2pins, \quad (3)$$

or 640 Gbits/s/pin, which is much larger than current solutions such as the 12.8Gbits/s/pin obtained in RAMBUS XDR2 [33]. Furthermore, Corona [7] employs half of pins used in typical RF solutions (4RFpins, 50Gbits/s/pin ranges), such as RFiof (details in section 4.1) can provide.

2.4 Comparing RF, 3Dstacking, and Optical

We now compare electrical/3Dstacking, optics, and RF under different aspects. In RF and optics, reports [15][21][35] indicate that the typical time range for up-conversion/down-conversion from data to light / RF waves and vice-versa delays is similar in optical and RF - about 200 ps. Furthermore, researchers [31][35] observe that optics presents a higher loss if compared to RF, since at this point, in terms of fabrication integration, optical and electrical are not as closer as RF and electrical.

The employed number of optical carriers is distant (4-12/64) from the theoretical limit(256), thus needing to mature if compared to RF. Confronting Frank Chang [21] and Kirman [31] studies, we observe that waveguides width/pitch to minimize crosstalk have a similar behavior in optics and RF. In terms of power and temperature, respectively an extra bus is needed for the optical laser power and optical circuits are reported [21] to be very sensitive, while RF follows CMOS. In terms of transceiver area, we notice that both technologies are reported [15][21][35] to use similar ranges.

We now compare RFiof and 3Dstacking. Regarding latencies, since researchers [20][21] indicate that RF-signals take around 100ps to travel 1cm-distance, we estimate that to travel 2.5cm - RFiof RFMC-to-rank distance, signals take around 250ps. However, in 3D-stacks systems, reports [19] indicate that to traverse 200 μ m-1000 μ m - equivalent to a 20-layer stack, signals take around 12ps, thus having 20x smaller delays when compared to RFiof. Regarding rank width, while typical 3Dstacking has 64-128 Byte-wide ranks, RFiof ranks are 8Byte-width ones, to keep typical rank width-size compatibility. Considering vertical RF-lines - as replacement of TSVs in 3D-stack systems - were employed to transfer larger width-ranks, they are likely to demand more RFpin related structures (microstrips and microstrip-to-coaxial interfaces), but not RFpads - replacement of I/O pads - since RFpads or equivalent are embedded and not respectively present either in RFiof or in 3Dstacking. In the latter, ranks are placed on a different 3D-layer, and when these and MCs are scaled, processor temperature is reported to be affected [11]. However, since RFiof is configured with typical ranks placed on the motherboard, ranks do not affect the processor temperature and heat dissipation.

3. RFIOF

We point out that the selection of RFiof elements was inspired in optics systems such as Corona [7], where each optical-pin and rank are connected via an optical fiber, versus an RFpin and coaxial cable in RFiof. Researching RF-based elements [17][21][35], our findings show that the structures proposed by Lameris et al. [17] fall in this category, once its RF structures have respective symmetric elements in counterpart optical ones such as in Corona [7].

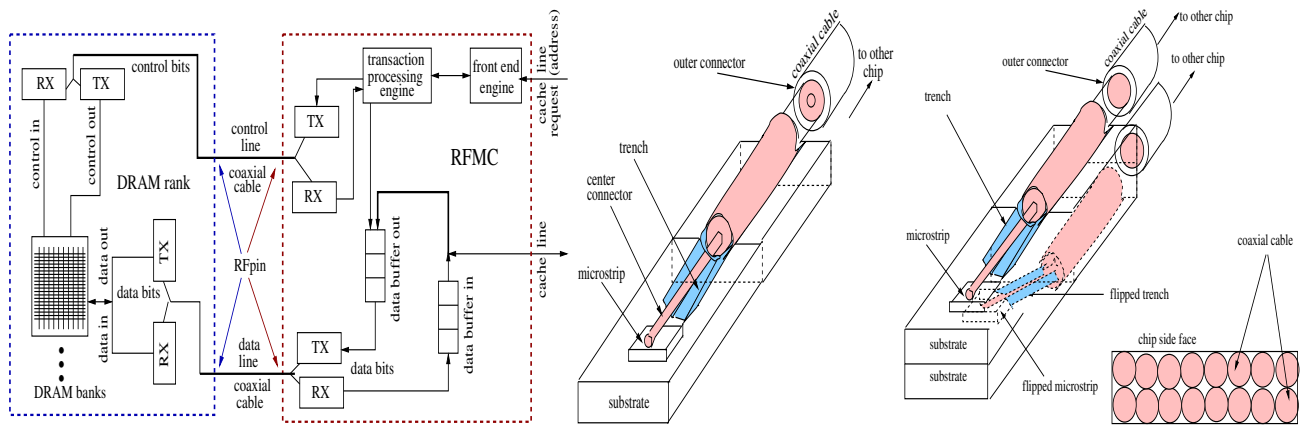


Figure 3: left to right: (a) RFiof memory design; (b) microstrip/trench ; (c) multiple cables interface and side view.

In order to connect processor and memory, RFiof employs the following methodological principles: (i) RF-design, (ii) minimization of components, (iii) low cost, and (iv) CMOS integration, which analysis, modeling and formulation, are discussed in the following sections.

3.1 Overview and Analysis

Regarding (i), the use of elements not designed according to RF-rules is likely to cause undesirable bandwidth degradation effects such as reflections, distortions, and dispersion effects at high-frequencies, thus causing signal loss and consequently bandwidth reduction. Since traditional I/O-pin-related structures are difficult to be implemented with controlled impedances, the previously bandwidth-degradation effects are likely to happen in this frequency-range.

Typical I/O pin structures, as illustrated in Figure 1a, have plenty of elements and are not matched in terms of impedances. (ii). Furthermore, PCB buses are long and significantly capacitive structures [18]. To address these effects in RFiof, impedances between two consecutive elements along the chain of the signal path are matched to avoid signal reflection at high frequencies. The proper impedance matching also reduces capacitive effects, which decreases reflection effects, thus minimizing bandwidth degradation. RFiof elements [17] are described along the next subsections.

To contrast with typical memory path elements such as MC and I/O pin elements, RFiof utilizes a RFMC, microstrip, microstrip trench, and a coaxial cable. Figures 1b and 3a respectively illustrate individual RFiof general scheme, its elements and their interconnection.

In RFiof, RFMCs are responsible for memory control, memory data transfers, and modulation of data/commands into RF, while the microstrip and microstrip-trench-to-coaxial interface are functionally similar to MC traces as well as an interface for the coaxial cable. And, the end of the path, we have TXs/RXs at the DRAM rank [17][25][29] which bring the signals from RF domain to digital.

Regarding (iii), RFiof employs a coaxial cable to connect RFMC and each rank, which is simple, modular, and individually upgradable if connected to faster memories, while cost-effective by reducing motherboard costs via elimination of PCB traces and vias connected to MCs. Moreover, the RF cable presents typical lower cost than a fiber.

About (iv), elements such as microstrips and interfaces - such as microstrip-to-trench interface, are very commonly employed in RF. Furthermore, these elements are traditionally fabricated in CMOS, which allows a better integration with traditional digital, when compared to optical elements.

By construction, a microstrip is designed with impedance and propagation constant as a function of the dimensions and dielectric material so that multiple carriers can be simultaneously transmitted while keeping low delays [29]. Its propagation delay is a function of the dimensions and the dielectric material as further described in section 3.5.

Figure 3b illustrates several interface elements. The microstrip-to-coaxial interface allows the RF signals to be transferred from the microstrip to the coaxial cable - selected as media as explained in the next paragraph. It is implemented according to the previously mentioned RF-design methodology, thus allowing dispersion control [17]. According to Lameres et al. [17][16], the microstrip trench is etched into the die substrate and then plated with conducted material, while the polygonal shaped trench guarantees mechanical alignment and supports the microstrip-to-coaxial trench [16]; both techniques and the Lameres [16] fabricated prototype demonstrate RFiof potential fabrication viability.

The coaxial cable - adopted due to its mobility, flexibility, upgradability, and low cost - connects the trench at the RFMC to ranks placed around the cores. Coaxial cables can be fabricated with very small diameters. For example, a 3mm-diameter, 400-GHz range one, is fabricated by Microcoax [27], and is appropriate for RFiof use.

3.2 RFiof signal path

Before showing RFiof signal path, we show that a typical MC signal path for purposes of reference. As shown in Figure 1a, at the flip-chip package interface, the signal path generated in the MC goes through the following path: MC, package trace, package via, repeaters, the structures which form the I/O pins - such as I/O pad, solder balls, and PCB pad-, and finally the signal reaches the PCB trace, and PCB via, followed by the same sequence in the opposite order when these signals traverse back from the rank to the MC.

In RFiof, TX/RX are placed at RFMCs and ranks (which were presumed as single chips). The path of the signals upon a cache request (Figure 1b) is as follows: at the RFMC TX, the digital address is converted to analog waves and, after they traverse the microstrip, they are sent through the microstrip/microstrip-to-coaxial interface, coaxial cable, and reach the rank RX - where the analog waves are converted back to digital, finally reaching the rank. The signal does traverse the same path in the opposite direction when a rank responds with the data burst. At the RFMC RX, it is converted down back and achieves the processor.

3.3 Ranks

We assume that the DDR3-ranks can be fabricated as sin-

gle chips (Figure 1b), so that the microstrip can be used to exchange requests and responses signals via TXs and RXs. The microstrip total length and cable length are kept at minimum to guarantee minimum delays and lower costs.

3.4 Extension: Proposal to Fit Many RFpins

We propose an extension of Lameres design [17][16], originally designed to work with frequencies up to 60 GHz, considering that these elements follow RF-modeling proposed by Frank Chang et al. [21][25], described in more details in section 3.5. These models presuppose elements designed for RF-frequency ranges, and have their fundamentals on the extensive RF-design and validation techniques, while very commonly utilized in the RF-area [21][25][34]. Furthermore, these models were vastly employed for different purposes (caches, memory) and at different ranges of frequencies [20][21][39], the latter which we envision in the proposed extension, after re-designed to operate at a larger frequency range, aiming to scale RFpins. RFiof employs microstrips which belong to the class of elements employed in these models. Regarding the used cable (table 2), it is designed to work properly at the targeted frequency, with appropriated construction parameter [27].

The proposed extension aims to scale RFpins, addressing the following restrictions: (i) typical coaxial cable dimensions are significant large when compared to typical package dimensions; (ii) each RFpin connects an RFMC to a rank. Before we describe the proposed extension, we point out that we presume typical package dimensions of 20mm x 20mm, and that since 3mm-cables coaxial cables are fabricated [27], thinner-diameter cables can be fabricated.

The extensions proposed are restricted to the microstrip and MEM-trench infrastructure. Starting from the set formed by the microstrip and micro-strip-to-trench structures showed in Figure 3b, we superpose another similar set, but flipped - illustrated on the left of Figure 3c. The 8 cables are arranged in rows, side by side, so that they can be fit in one package side (20mm - right of the Figure 3c), allowing 32 coax cables, which connect the 32 RFMCs to the (32) respective ranks.

3.5 Delay Modeling and Formulation

We start this subsection briefly describing about RFiof circuitry and its modeling. We further explain how the circuitry and modeling incorporate reduction of transmission errors and noise margin. We also explain what are the essentials of the modeled RF circuitry and how the models behave with technology improvement.

Generically regarding RF circuits, researchers [34] report that RF signals are mostly represented by its LC (inductive-capacitive) part, and that inductors [21] – dominant in TX / RX circuits – are inversely proportional in size to the operational frequency. Thus, according to ITRS [21], due to frequency scaling and consequent carrier frequency scaling, TX/RX area also scales down. Similarly, according to [21], the number of channels available is also expected to scale due to the availability of faster transistors.

As previously mentioned and justified in section 3.4, we assume RF-circuitry modeling and scaling proposed by Frank Chang et al. [21][25] are valid for RFiof, which is also the same methodology adopted by other reports [21][20][35]. In these models, modulation and line separation are taken into account in order to keep a low bit error rate (BER). Furthermore, according to these models, maximum data rate and number of available channels scales with technology (rule of thumb: maximum data rate as half of the maximum carrier). In addition, these models also take noise margin reduction and differential transmission into account – via doubling the

technology (nm)	45	32	22
carriers	10	12	14
data rate per band (Gbits/s)	7	8	10
total data rate per wire (Gbits/s)	70	96	146
space between carriers (GHz)	28	32	36
power (mW)	60	72	84
energy per bit (pJ/bit)	0.85	0.75	0.6
area (TX + RX) (mm ²)	0.0115	0.0119	0.0123
area / (data rate) (um ²)/Gbits/s	164	124	88

Table 1: replicated results from modeling RF technology obtained from [13][21]

number of lines to minimize crosstalk effects as further described in section 4.1.

Moreover, this modeling also envisions that dispersion and distortion levels of RFiof structures are tolerated accordingly. The models incorporated in this methodology were validated and prototyped, as well as they are valid for transmission lines such as microstrips employed in RFiof, and follow ITRS [13][21][35]. Typical parameters provided by these models are data rates per carrier, space between carriers, total data rate per wire, as well as area and power of the TX/RX RF circuits, as illustrated in Table 1.

We change to the delays estimation in RFiof. The overall delay of RFiof is given by the summation of the delays over the microstrip, trench, the coaxial cable, and the other side of the microstrip again, but on the other chip. To calculate the microstrip delay, we use the equation derived from [29]:

$$T_{\mu pd} = 1.016\sqrt{(0.475 * \epsilon_r + 0.67)ns/foot} \quad (4)$$

where $T_{\mu pd}$ is the microstrip delay and ϵ_r is the dielectric coefficient of the microstrip. Regarding the coaxial propagation delay, the following equation [29] is valid:

$$T_{coaxialpd} = 1.016\sqrt{(\epsilon_r)ns/foot} \quad (5)$$

where $T_{coaxialpd}$ is the coaxial delay and ϵ_r is the dielectric coefficient of the coaxial cable. The rest of the delays is discussed in the following section.

4. EXPERIMENTAL SECTION

In this section, we determine RFpin counts scaling for different memory technologies and types, using a similar methodology to the proposed by Marino [23], but applied to I/O pins. Furthermore, we compare RFpin count with other technologies such as optics, electrical, and 3D-stacking. In the sequence, we employ the methodology proposed in [24] to estimate area and power architectural benefits of replacing MCs with RFMCs in RFiof. After that, we discuss the methodology and bandwidth/speedups results obtained when scaling RFMCs, as well as observe latency reduction via transaction queue occupancy and duration reduction.

4.1 RFpin count / dimensions: matching current ranks and future memory scaling

In order to avoid circuit replication at the rank, buffering control, and data bits in both rank/processor sides, we propose creating dedicated RFpins for control and data in order to keep DRAM circuitry as close to the original as possible.

Employing a 22-nm technology and the previous RF models (table 1), there are 14 carriers, statically allocated with 36GHz-inter-channel space (low BER), and 10 Gbits/s-data-

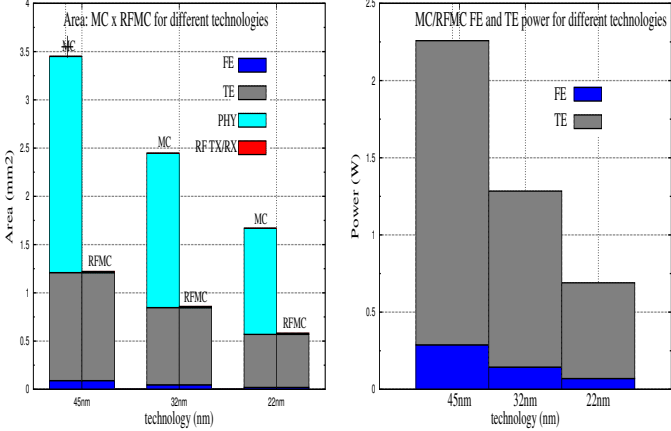
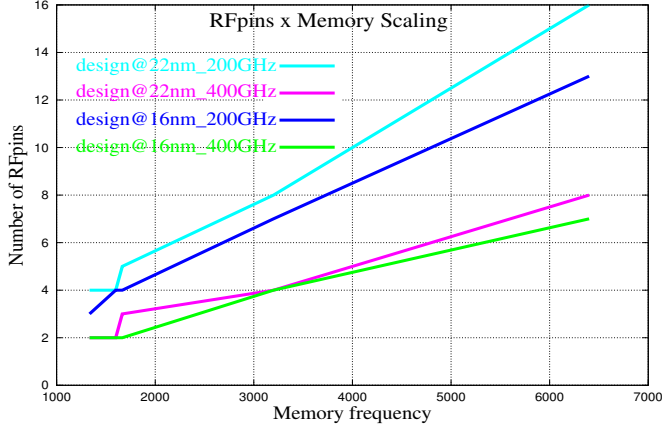


Figure 4: top to bottom, left to right: (a) RFpins versus memory scaling; FE/TE (b) area and (c) power

rate per carrier. Given the coaxial cable maximum upper limit frequency (400GHz), half of that is available to the carriers (Nyquist): thus 5 carriers, each with 10 Gbits/s-data-rate, provide an RFMC data rate budget of 50 Gbits/s.

To illustrate the design of the RF interface, we particularly chose a DDR3 memory due to its large employment in general PCs and due to its significant pin counts (180 - 240). Once the delays through TX/RX are very small – within 200-picoseconds range [21] – when compared to the memory timing operations, they are not considered in the following formulations. The module particularly chosen is the Micron MT41K128M8 of 1GB (64 data bits, 1333 MT/s, table 2), with significant pin counts (180 - 240), and experimented in section 2.1. To determine RFpin counts we define:

$$RFpins = \text{number of I/O pins per RFMC} \quad (6)$$

and the memory throughput is defined as:

$$m_throughput = m_cycle * tot_bits_transferred, \quad (7)$$

where m_cycle is the memory cycle. Using m_bits as the amount of memory bits transferred in one memory cycle, we have in the sequence :

$$RFpins_for_data = \text{floor}(data_m_bits / m_throughput) \quad (8)$$

Then, using modulation and high-speed signaling to transfer memory bits in equation (2), we have:

$$m_throughput = m_cycle * RF_data_rate * n_carrier \quad (9)$$

And, for data bits (data - d), we then have:

$$RFpins_d = \text{floor}(d_m_bits / d_m_throughput) \quad (10)$$

where data refer to data bits, such as a burst. Similarly, for control bits (control - c):

$$RFpins_c = \text{floor}(c_m_bits / c_m_throughput) \quad (11)$$

And finally,

$$RFpins = RFpins_d + RFpins_c \quad (12)$$

To determine the number of RFpins needed, we determine the total amount of data bits transferred in one memory cycle, which we define as tot_bits :

$$tot_bits = \text{total amount of bits in } m_cycle \quad (13)$$

We now exemplify RFpin count calculation for the target rank. Inspecting the rank and similar ones in Micron DDR3 catalogs [28], except voltage, ground, and not-connected pins, the total number of pins effectively used for data transmission in a rank access - composed by a sequence of operations on the control and data busses - is around 123 bits (around 50%, with 64 for data, 59 for control of a total of 240 pins). Examining rank pin usage and timing, equation (13) shows that in one memory cycle we can have:

$$tot_bits = (1/1333MT/s) * 5carriers * 10Gbits/s, \text{ or } \quad (14)$$

$$tot_bits = 37.5bits; \text{ floor}(37.5) = 37bits, \quad (15)$$

i.e., 37 bits can be transferred in one memory clock period, along one RFpin. Hence, 2 RFpins are necessary to carry all the 64 data bits and 2 RFpins for the 59 control bits needed, for a total of 4 RFpins. This RFpin count is scalable and has a similar magnitude to Corona 2-optical pin-count showed by Vantrease et. al [7]. Figure 4a shows the result of RF scaling (combination of equations 3 to 10) with memory frequency scaling at 16nm; from this figure, we observe low-magnitude RFpin counts for different memory generations, even for memories with larger clock frequencies than DDR4 ones. In addition, disregarding the 400GHz-upper-limit, we observe RFpin-scalability equivalent to 2-optical pins.

Compared to traditional memory solutions, RFiof respectively presents a pin reduction of 16x and 24x if compared to RAMBUS XDR2 and Intel FBDIMM. Compared to optical-pins, RFiof has 2x more I/O pins (4 RFpins) or the same count if the 400GHz upper limit is disregarded.

Analyzing ITRS predictions [13], we have found that around 512 (rounded) pins are exclusively dedicated to memory, once there are pins related to other elements (for example, PCI). Assuming a typical DDR3 240-pin budget and the area estimation (50%), we can potentially save up to 46.9% $((123+123)/512)$ of the die area dedicated to the I/O pins. Considering applying this RFiof technique to current 2-4MC-microprocessors, potentially up to 492 I/O pins, which correspond to 4.920000 mm^2 of area saving can be obtained, with the typical 1000 um^2 per pin [13]. Furthermore, assuming similar pad-to-pin rates, similar area pad reduction could be obtained. Moreover, this analysis overestimates the number of control signals simultaneously used (clock included), which optimization is not presented due to space reasons. Finally, the investigation of having both control / data lines buffered and sequential transmission over a unique microstrip line are left as a future investigation.

4.2 Area and Power Analyses

In this section, we analyse area/power aspects of MC / RFMC, rank, and RF interconnection. Before the analysis, we list the typical MC composition: (i) front engine (FE), which processes cache requests, (ii) transaction engine (TE), which transforms memory requests into control / data memory commands, and (iii) physical transmission (PHY), constituted by control / data physical channels [37].

To determine the RFiof architectural benefits of replacing MCs with RFMCs, we employ Marino's strategy [24]. This strategy focuses in two aspects: (i) area, (ii) and power benefits. In both of these aspects, McPAT tool [37] is employed to determine area and power of FE/TE present in both MC and RFMC, as well as for the MC PHY area part. However, to determine RFMC PHY area dimensions, the proposed

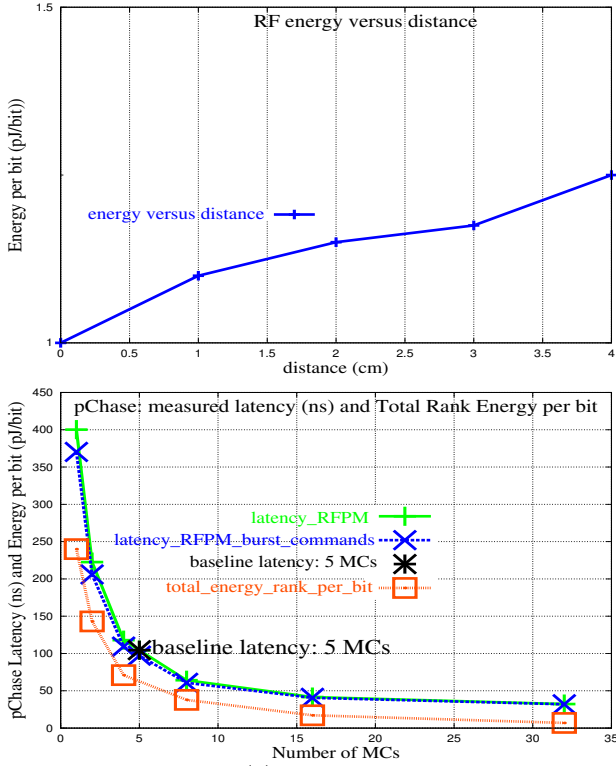


Figure 5: left to right: (a) energy versus distance replicated from [35]; (b) RFiof total rank energy and pChase latency

strategy employs RF RX/TX area dimensions obtained via Frank Chang et al. circuitry modeling estimations [21][35], such as the ones listed in Table 1.

4.2.1 RFMC versus MC area (baseline)

The proposed methodology is applied to the (i) MC versus RFMC area comparative aspects. As a result, we observe in Figure 4b that for different technologies, the area of one RFMC corresponds to around 36.5% of the area of one MC, i.e., considering the MC area as area budget, we can fit up to 2.8x more RFMCs on the die, which means that, for the multicore baseline (5 MCs - section 2.1) MC-area, we can have up to 14 RFMCs within this same area budget.

4.2.2 RFiof TX/RX Rank area

To estimate area dimension of the TX/RX area at the rank, we employ a similar methodology to the one used in previous subsection. While the results of this estimation indicate an area of about 0.015-0.0123 mm² - a small area overhead, considering typical fabricated memory die area of 50 mm² [28]. To further broaden this estimation, given the RF-memory prototype reported by Byun et al. [9], which has TX/RX area of about 0.094 mm², the overhead of this area compared to the total chip area is still not significant.

4.2.3 MC versus RFMC power comparison

We organize the following analyses to identify RF power and energy benefits of RFiof and comparatively analyse it to the respective MC counterpart in each part of the memory path: (1) MC power comparison; (2) RFiof interconnection energy; and (3) rank power and total rank energy.

As previously mentioned in section 4.2.1, we adopt Marino's methodology [24] to compare FE/TE power in MC versus RFMC, since both are either present in RFMC and MC (obtained via McPAT tool [37]). These magnitudes are illustrated in Figure 4c, where we observe that for different

technologies (45, 32, and 22nm), FE/TE power decrease as technology improves - justified by the improvement of technology as the transistors size shrink as mentioned in [37].

Concentrating on the MC PHY power, most represented by the amount of bits transferred, it is the most power relevant when compared to the FE and TE. We envisioned this as a component of the dynamic energy, which includes I/O pin power, and is analyzed in the following section.

4.2.4 RFiof interconnection energy

To perform the interconnection energy determination, we employ the power versus distance projection from Tam et al [35] which is replicated in Figure 5a, and apply it for the average distance between RFMCs-ranks, estimated as 2.5 cm. As a result, we obtain 1.2 pJ/bit for the interconnection energy. To determine the MC interconnection energy, we measure the PHY power provided by McPAT [37] and divide by the amount of transferred bits, in a similar experiment as the one performed in section 2.1; we obtained around 6 pJ/bit. Thus, we estimate that the interconnection energy savings are about 80%. With a similar strategy as the one utilized when performing RFMC area comparison (section 4.2.1), we estimate that we can fit up to 25x more RFMCs, which alternatively represents an architectural benefit. Since the area benefits obtained in the section 4.2.1 are smaller (equivalent to 14 RFMCs), we conservatively assume the latter as the dominant and do not determine the architectural performance benefits related to power.

4.2.5 Rank Power and Total Rank Energy

Since TX/RX elements are part of RFiof transmission, RFpin power is consumed as a replacement of I/O pin termination power. Using a similar approach as the one used to compare RFMC versus MC power, combined to Micron DRAM sheet power, we determine the rank power. As a result, we can save up to 6.7% of the DRAM power in RFiof.

In order to determine the total rank energy usage, we performed the following calculation:

$$\text{memory energy} = \text{total power} / \text{total bandwidth} \quad (16)$$

To obtain the rank power, we employ Micron data sheet parameters [28] combined to DRAMsim [8], which provides the total number of memory accesses. Total rank energy contemplates the total dynamic and static energy of the set formed by all employed ranks. Bandwidth measurement was obtained via experiment with similar settings as performed in section 2.2, with different RFMC/MC counts. The results of this experimentation are shown in Figure 5b, which demonstrates that memory energy usage decreases in up to 43.9% compared to the baseline (baseline reference with 5 MCs, as explained in section 2.1) as we increase MC counts, given that the high memory bandwidth scaling obtained via RFMC scaling is proportionally higher than power scaling (equation 16). An important observation is that although energy levels usage showed are significantly high, i.e. up to 240 mW/bit, these magnitudes are at these levels due to the DDR3-rank model selected. Since RFiof is compatible with DDR-memory family, it could certainly be applied to low power ranks, such as LPDDR2 ones.

4.3 Methodology, Bandwidth, and Speedups

Before describing the methodology, we observe that we do not include optical modeling due to the fact that, for the distance traversed, typical optical delays do have similar magnitudes to RF [15][21][35], which would result in similar bandwidth / speedups / latency behavior (adopting the same settings for other hardware elements).

We model RFiof by employing M5 [30] and DRAMsim

Core	4.0 GHz, OOO-Core, 4-wide issue, turnament branch predictor
technology	22 nm
L1 cache	32kB dcache + 32 kB icache; associativity = 2 MSHR = 8, latency = 0.25 ns
L2 cache	1MB/per core ; associativity = 8 MSHR = 16; latency = 2.0 ns
RF crossbar	latency = 1 cycle
RFMC trans. queue	1 to 32 RFMC; 1 MC/core, 4.0GHz, on-chip, close page mode buffer size = 32/MC
Memory rank	DDR3 1333MT/s, 1 rank/MC, 1GB, 8 banks, 16384 rows, 1024 columns, 64 bits, Micron MT41K128M8 [28] tras=26.7cycles, tcas=trcd=8cycles
Microstrip: lenght, delay	1.0 cm, 0.06ns
Coaxial cable: lenght, delay	2.5 cm, 0.125ns

Table 2: modeled architecture parameters

[8] simulators . Memory transactions are generated by M5 and captured by multiple MCs/RFMCs in DRAMsim, which respond with the result of the memory transaction.

To evaluate RFMC scalability, we observe that our experimentation covers different core:MC ratio (1:1/32, 1:1/16, until 1:1), or put differently, with different RFMC counts (1 to 32) for 32 cores. In addition, we restate that the baseline has 5 MCs (discussed in section 2.1). In order to evaluate MC scalability, we have employed the most conservative addressing mode by interleaving cache lines along the RFMCs, so that we do not take advantage of locality. Moreover, in order not to take advantage of locality benefits, we have employed closed page mode (server environment) in all of the experiments [8]. The memory timing parameters are based on rank previously analyzed (section 2.1, 1GB DDR3, Micron model MT41K128M8 [28]).

To guarantee enough pressure on the memory system, we have utilized an OOO processor model. The processor modeled follows a clustered architecture, where we have one core per L2 slice, i.e., private L2 slices in order to avoid cache sharing effects. The ISA employed is based on Alpha processor, configured as a 4-way issue OOO core as typical current processors [3]. Furthermore, we presumed a banked and scalable L2 MSHR structure [40]. We assumed 1MB/core as an L2 cache slice size to reflect current OOO processors. L2 slices communicate through an 1-cycle RF-crossbar configured with same latency assumption of Frank Chang [21] study: 200ps of TX-RX delay, plus the rest of the cycle to transfer 64 Bytes using high speed and modulation. We obtained cache latencies from Cacti [5] and adopted MSHR counts for each L2 slice similarly to the 3D-stack study by Loh [18] reflecting configuration of a real processor.

Regarding memory delays, we have utilized typical two cycles for command-duration period and eight cycles for a burst-duration; due to the speed-of-light property of RF, we estimate that the command-duration delays are reduced from two to one cycle and the bursts, from eight to one cycle. PCB delays are not included in the baseline modeling since we found a broad variety of magnitudes; due to that, the baseline measurements, such as bandwidth / speedups, are closer to the ideal case, i.e., RFiof-likely bandwidth results are better than ones achieved here.

We estimate the coaxial-cable length size of 2.5cm and total microstrip length size (both microprocessor and rank) around 1.0 cm, with microstrip / coaxial cable delays respectively using equations (4) and (5), section 3.5. As a

Benchmark	Input Size	read:write, MPKI
Copy, Add, Scale, Triad (STREAM)	4Mdoubles per core, 2 iterations	2.54:1 , 54.3
pChase	64MB/thread, 3 iterations, random	158:1 , 116.7
Hotspot (Rodinia)	6000 x 6000, 3 iter.	2.5:1 , 12.5
CG: Conjugate Gradient (NPB)	Class A, 3 iterations	76:1 , 16.9
MG:Multigrid (NPB)	Class A, 3 iterations	76:1 , 16.9
SP: Scalar Pentad (NPB)	Class A, 2 iter.	1.9:1 , 11.1
FT: Fourier Trans. (NPB)	Class A, 3 iterations	1.3:1 , 6.8

Table 3: benchmarks and input sizes

result, we obtain about 0.06ns and 0.125ns in terms of delays using the typical dielectric constant magnitudes of 4.5 and 2.1 from [17], respectively for the microstrip and coaxial cable. These delays were incorporated into the modeled interconnection in M5. To finalize, table 2 summarizes all parameters we employed in the simulation environment.

Using Loh’s criteria [18], we selected memory bandwidth-bound benchmarks, focusing on the ones with a significant number of misses per kiloinstructions (MPKI) to stress the memory system. Above the selected benchmarks, we have (i) STREAM [26] suite, which we decompose in its four sub-benchmarks (Copy, Add, Scale, and Triad); (ii) PChase [32] with pointer chase sequences randomly accessed; (iii) Hotspot from Rodinia suite [38]; (iv) Conjugate Gradient (CG), Scalar Pentadiagonal (SP), Multigrid (MG), and Fourier Transform (FT), these all from NPB [2]. STREAM and pChase are designed to evaluate bandwidth, while the latter also evaluates latency. The selected NPB applications reflect the bandwidth aspect of the HPC challenge [2].

Table 3 summarizes the benchmarks experimented, input sizes, read-to-write rate, and L2 MPKI obtained in the experiments. In all benchmarks, the parallel regions of interest were executed until completion. All the input sizes are larger than the total memory size, which guarantees that all the memory space is stressed. The average results were calculated based on harmonic average.

4.3.1 Bandwidth, Speedups, and Related

We define the following terminology:

- baseline: MC scalability under I/O pin constraints. The baseline has 5 MCs, and 32 cores, according to the methodology employed in section 2.1.
- RFiof: defined as the proposed version, i.e., evaluating the RFMC scalability.
- RFiof_burst_command: difference between RFiof plus RF latency benefits, and RFiof.
- RFiofa: defined as the RFiof version with the same area budget as the baseline to explore its architectural benefits in terms of higher RFMC counts (RFMC area saving). It is obtained by RFiof extrapolation and has 14 RFMCs (discussed in section 4.1).
- RFiofa_burst_command: difference between RFiofa plus RF latency benefits, and RFiofa (similarly, 14 RFMCs).

Figure 6 shows the bandwidth obtained in the experimentation for different core:MC ratio (1:1/32, 1:1/16, until 1:1), or put differently, with different RFMC counts. For all the STREAM benchmarks and pChase, which were designed to measure bandwidth magnitudes, and for different core:MC ratios, bandwidth was improved; RFiof, RFiofa, respectively provide up to 7.2x and 4.2 more bandwidth than the baseline due to the larger RFMC counts available, allowing more memory transactions to be processed simultaneously, which also can be noticed through a lower average transaction queue occupancy and duration (right side of Figure 6a).

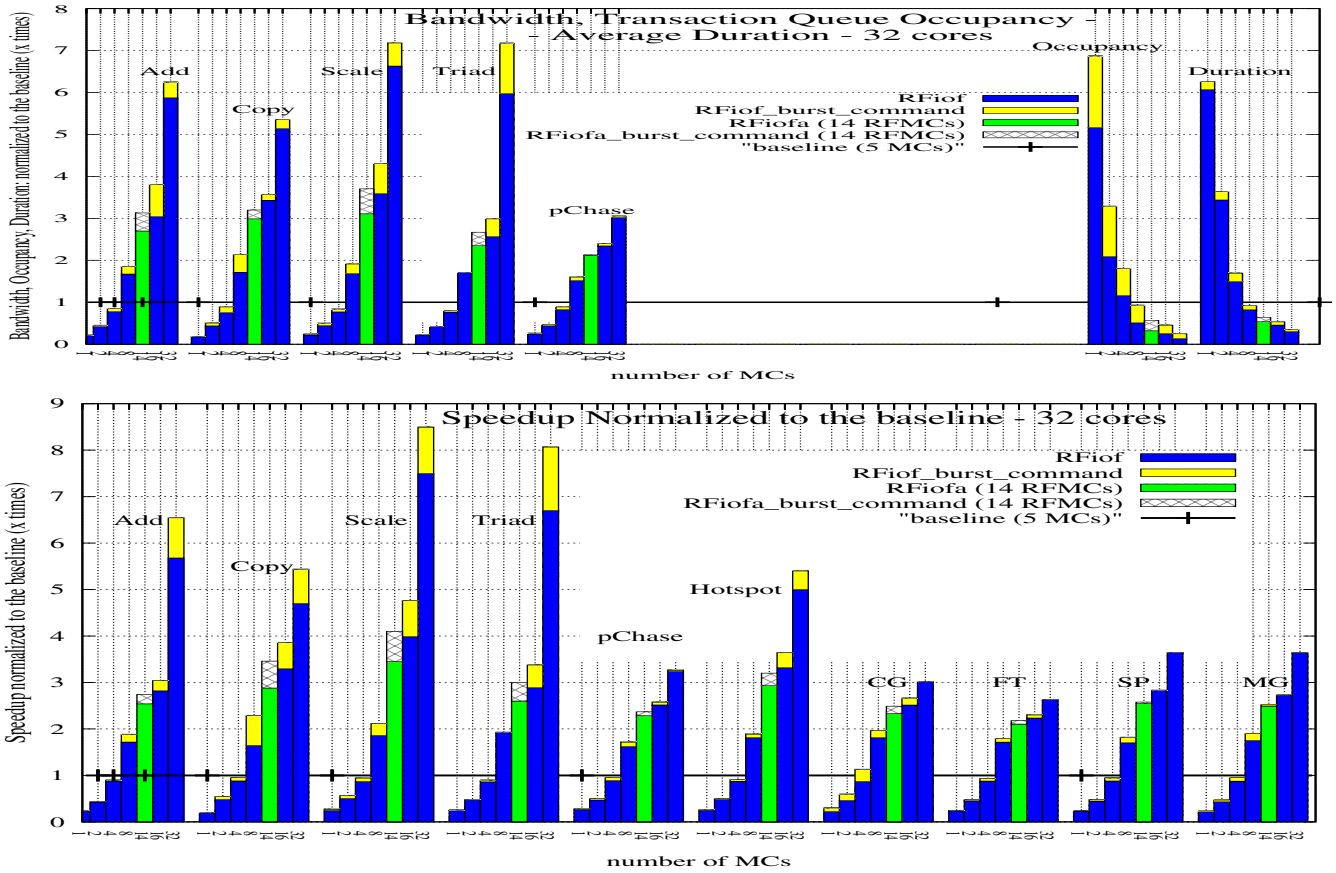


Figure 6: left (a) bandwidth, transaction queue occupancy and duration; right: (b) speedups; RFiof: RFMC scalability; RFiofa: RFiof under area budget; RFiof_burst_command/RFiofa_burst_command: RFiof and RFiofa plus RF latency benefits.

We only show the transaction queue average occupancy and the duration for the most memory intensive benchmarks - STREAM and pChase. The larger RFMC-count allows to increase the number of memory transactions simultaneously served, while transactions queues become shallower and less occupied (on the right of Figure 6a). Compared to the baseline, transaction queue occupancy is respectively reduced of about 86% and 68% for RFiof and RFiofa. Furthermore, the larger RFMC-counts affect the duration of one transaction: as showed in Figure 6a, the average duration is decreased by up to 60% and 40% for RFiof and RFiofa, with the baseline as reference; alternatively, as the RFMC-counts increase, the memory system overall latency decreases, which also confirms bandwidth scaling. Figure 4e shows the average pChase memory latency RFiof; compared to the baseline, this latency is reduced by around 69% through RFMC scalability and up to 69.5% when the high-speed transmission benefits are included.

Figure 6b illustrates speedups obtained across the benchmarks for different core:MC ratio (32:1, 32:2, until 32:32), i.e., different RFMC counts. For all benchmarks, we observe that speedups increase in the same proportion as a result of the larger RFMC availability. For STREAM, RFiof and RFiofa are respectively up to 8.6x and 5.6x faster than the baseline. Similar scaling trends are obtained for pChase, Hotspot, CG, and FT; for these benchmarks, RFiof respectively achieved up to 3.23x faster for pChase, 5.0 x for Hotspot, 3.01x faster for CG, 2.63x for FFT, 3.64x for SP, and finally 3.64x for MG, when compared to the baseline version. Accordingly, RFiofa followed a similar improvement trend. The largest bandwidth/speedup improvements occur for the STREAM suite due to its access pattern (stream) and large MPKI magnitudes (Table 3).

We now concentrate on the high-speed RF latency ben-

efits. Regarding commands duration and burst we observe bandwidth improvements of up to 25%. Similarly, speedups are improved, for all the selected applications; in this case, speedups are improved by up to 20.4% as illustrated in Figure 6b. In this case, the transaction average duration and occupancy (in this case accounted by decreasing the yellow bar from the total) observed on the right of Figure 6a, are reduced by up to around 67% and 20%. The same trend is also valid for RFiofa, in terms of bandwidth (20%) and speedup (18%). In terms of RF latency decrease, pChase indicates a maximum reduction of about 7.5% (Figure 4e). Moreover, for all the benchmarks evaluated, as the number of RFMCs grows, the RFMC scalability benefits (RFiof) are more dominant than the latency ones (burst_command versions), because the transaction queue contention reduction is larger than the latency reduction.

We observe that some benchmarks exhibit traffic imbalance between memory controllers in interleaved mode and a speedup saturation for higher RFMC counts. After deeply investigating the simulation infrastructure statistics, we notice that some L2 slices presented significantly different miss rates as RFMC-count is scaled; this context presents many similarities to the churn phenomenon described by Loh [18] when scaling MSHRs, which we leave as further investigation. Furthermore, larger input sizes could potentially address SP and MG speedups saturation after 8/16 RFMCs, since we restrict M5 address space size to 2GB.

5. RELATED WORK

10 TB/s-bandwidth Corona [7] optical memory system (160 GB/s/MC) was designed aiming low energy levels (7.8 nJ/bit) per memory channel access, and most importantly, with only 2 optical I/O pins per optical memory. Although conceived for CMOS, RFiof has similar order of number of

pads (4 RFpins), disregarding the 400GHz upper limit.

The reconfigurable CDMA RF memory bus by Kim et al [14] targets I/O pin-count reduction and bandwidth. However, this solution was not interfaced to MCs, neither to supply the multicore-era bandwidth demands. Moreover, RFiof adopts FDM, reported [25] to present higher bandwidth than CDM used in this CDMA bus. Given this CDMA bus [14], the RF-overlaid with mesh in [20][21], and Tam's [35] RF-in-future microprocessor design, RFiof employs an equivalent approach regarding RF theory/circuitry modeling.

The DIMM Tree architecture [39] targets off-chip memory, investigating the trade-offs between a multi-drop rank latency versus the RF single-drop latency, as well as the RF bandwidth supplied to each rank versus the number of ranks. While sharing RF, RFiof provides a significantly lesser pin count (around 4RFpins) than DIMM Tree (39 pins). Moreover, DIMM Tree focuses on rank scalability using the same RFMC, while RFiof on RFMC scalability.

Marino [24] proposed an on-package RF-memory organization targeting MC-power reduction. While both employ RF, RFiof focuses on I/O pin scalability to explore RFMC scalability, aiming bandwidth and performance. As a follow up paper, Marino [22] extended this architecture to focus on I/O pad scalability; to contrast with the later, which focuses on package-pad reduction, RFiof focus also in I/O pin reduction, which allows larger RFMC scalability.

6. CONCLUSION AND FUTURE PLANS

We have proposed RFiof memory organization as an approach to the I/O pin problem. In RFiof, MC and typical I/O pins are replaced by RF-designed apparatus, which include RFMCs, RFpins, RF TX/RX, microstrip/-to-coaxial interface, and a coaxial cable. RFiof advantages are manyfold: (i) by removing the MC I/O pin constraints via a scalable RFpin-count, we demonstrate high bandwidth by scaling RFMCs, thus improving performance, (ii) die area and (iii) power/energy reduction, (iv) DDR-family compatible, (iv) and a cost-design alternative to optical systems.

As future research points, we plan to evaluate RF benefits when communicating to 3D-stack memories, as vertical RF-TSVs viability improve. Although RFiof is DDR-compatible, we plan to develop a dedicated rank, to further explore its performance and power benefits.

7. REFERENCES

- [1] Moore's Law, 40 years and Counting. Accessed date: 09/10/2011 ; <http://download.intel.com/technology/silicon/Interpack>.
- [2] NAS Parallel Benchmarks. Accessed date: 11/11/2012 ; <http://www.nas.nasa.gov/Resources/Software/npb.html/>.
- [3] AMD Reveals Details About Bulldozer Microprocessors, 2011. accessed date: 11/10/2012 - http://www.xbitlabs.com/news/cpu/display/20100824154814_AMD_Unveils_Details_About_Bulldozer_Microprocessors.html.
- [4] The Era of Tera: Intel Reveals more about 80-core CPU. Accessed date: 08/27/2011 ; <http://www.anandtech.com/cpuchipsets/showdoc.aspx?i=2925>.
- [5] CACTI 5.1. Accessed Date: 10/20/2012; <http://www.hpl.hp.com/techreports/2008/HPL200820.html>.
- [6] The Push of Network Processing to the Top of the Pyramid. Accessed date: 07/21/2012 ; <http://www.cesr.ncsu.edu/ancs/slides/eathertonKeynote.pdf>.
- [7] Dana Vantrase et al. Corona: System Implications of Emerging Nanophotonic Technology. In *ISCA '08*, pages 153–164, Washington, DC, USA, 2008. IEEE Computer Society.
- [8] David Wang et al. DRAMsim: a memory system simulator. *SIGARCH Comput. Archit. News*, 33(4):100–107, 2005.
- [9] G. Byun et al. An 8.4Gb/s 2.5pJ/b Mobile Memory I/O Interface Using Bi-directional and Simultaneous Dual (Base+RF)-Band Signaling. *IEEE*, 2011.
- [10] GT 200. Accessed date: 08/27/2012 ; <http://www.hardwaresecrets.com/>.
- [11] Healy, M et al. A Study of Stacking Limit and Scaling in 3D ICs: An Interconnect Perspective. In *Electronic Components and Technology Conference*, pages 1213–1220, Washington, DC, USA, 2009. IEEE Computer Society.
- [12] Intel Fully Buffered DIMM. Accessed date: 08/26/2012 – http://www.intel.com/.../FBDIMM/.../Intel.FBD_Spec.Addendum_rev_p9.pdf.
- [13] ITRS HOME. Accessed date: 09/12/2012 ; <http://www.itrs.net/>.
- [14] Kim, J. et al. Reconfigurable Memory Bus Systems using Multi-Gbps/pin CDMA I/O Transceivers. In *ISCAS*, volume 2, pages 33–36, Bangkok, Thailand, 2003. IEEE.
- [15] Kobrinsky M. J. et al. On-Chip Optical Interconnects. *Intel Technology Journal*, 8(2):129–142, 2004.
- [16] LaMeres B. J. et al. Novel 3-D Coaxial Interconnect System for Use in System-in-Package Applications. *IEEE Transactions on Advanced Packaging*, 33(1):37–47, 2010.
- [17] LaMeres B.J., McIntosh C. Off-Chip Coaxial to Microstrip Transition Using MEMs Trench. *3D/SiP Advanced Packaging Symposium*, 33(1), 2008.
- [18] Loh, Gabriel H. 3D-Stacked Memory Architectures for Multi-core Processors. In *ISCA '08*, pages 453–464, Washington, DC, USA, 2008. IEEE Computer Society.
- [19] G. L. e. a. Loi. A thermally-aware performance analysis of vertically integrated (3-D) processor-memory hierarchy. In *Proceedings of the 43rd annual Design Automation Conference*, pages 991–996, New York, NY, USA, 2006. ACM.
- [20] M-C. Frank Chang et al. Power reduction of CMP communication networks via RF-interconnects. In *MICRO'08*, pages 376–387, Washington, DC, USA, 2008. IEEE.
- [21] M. Frank Chang et al. CMP Network-on-Chip Overlaid With Multi-Band RF-interconnect. In *HPCA*, pages 191–202, 2008.
- [22] Marino, M. D. On-Package Scalability of RF and Inductive Memory Controllers. In *Euromicro DSD*. IEEE, 2012.
- [23] Marino, M. D. RFiop: RF-Memory Path To Address On-package I/O Pad And Memory Controller Scalability. In *ICCD, 2012, Montreal, Quebec, Canada*. IEEE, 2012.
- [24] Marino. M.D. and Skadron K. Reducing Power and Area by Interconnecting Memory Controllers to Memory Ranks with RF Coplanar Waveguides on the Same Package. In *WEED Workshop, in conjunction with ISCA*, 2011.
- [25] Mau-Chung Frank Chang et al. Advanced RF/Baseband Interconnect Schemes for Inter- and Intra-ULSI Communications. 52:1271–1285, Jul 2005.
- [26] McCalpin, John D. Memory Bandwidth and Machine Balance in Current High Performance Computers. *IEEE TCCA Newsletter*, pages 19–25, Dec. 1995.
- [27] Leading the way in transmission line solutions. Accessed date: 08/13/2011 ; <http://www.micro-coax.com/>.
- [28] Micron manufactures DRAM components and modules and NAND Flash. Accessed date: 12/28/2012 ; <http://www.micron.com/>.
- [29] A practical resource covering the fundamental principles of microwave design. Accessed date: 10/30/2012 - <http://www.microwaves101.com/>.
- [30] Nathan L. Binkert et al. The M5 Simulator: Modeling Networked Systems. *IEEE Micro*, 26(4):52–60, 2006.
- [31] Nevin Kirman et al. Leveraging Optical Technology in Future Bus-based Chip Multiprocessors. In *MICRO'06*, pages 492–503, Washington, DC, USA, 2006. IEEE Computer Society.
- [32] The pChase Memory Benchmark Page. Accessed date: 05/22/2011 ; <http://pchase.org/>.
- [33] Rambus. Accessed date: 11/14/2012 ; <http://www.rambus.com/>.
- [34] Richard T Chang et al. Near Speed-of-Light Signaling Over On-Chip Electrical Interconnects. *Journal of Solid-State Circuits*, 38(5):834–838, 2003.
- [35] Sai-Wang Tam et al. RF-Interconnect for Future Network-on-Chip. pages 255–280, 2011.
- [36] Shane Bell et al. TILE64TM Processor: A 64-Core SoC with Mesh Interconnect. pages 88–90. IEEE, 2008.
- [37] Sheng Li et al. McPAT: an integrated power, area, and timing modeling framework for multicore and manycore architectures. In *MICRO'09*, pages 469–480, New York, USA, 2009. ACM.
- [38] Shuai Che et al. Rodinia: A benchmark suite for heterogeneous computing. In *IISWC*, pages 44–54. IEEE, 2009.
- [39] K. e. a. Therdsteerasukdi. The dimm tree architecture: A high bandwidth and scalable memory system. In *ICCD*, pages 388–395. IEEE, 2011.
- [40] Tuck, James et al. Scalable Cache Miss Handling for High Memory-Level Parallelism. In *MICRO'06*, pages 409–422, Washington, DC, USA, 2006. IEEE Computer Society.